Anodized Aluminum Oxide Thin Films for Room-Temperature-Processed, Flexible, Low-Voltage Organic Non-Volatile Memory Elements with Excellent Charge Retention

Martin Kaltenbrunner, Philipp Stadler, Reinhard Schwödiauer, Achim Walter Hassel, Niyazi Serdar Sariciftci, and Siegfried Bauer*

Despite considerable achievements in organic electronics, including examples of complex integrated circuits,[1] transistor matrix arrays for optical[2] and Braille displays,[3] image scanners,[4] and large-area electronic skin,[5] non-volatile organic memories remain underexploited.[6] Even at the lower end of the market, where potential applications are smart cards, wireless tags, and large-area sensors, no non-volatile memory that meets the minimum requirements in terms of access time, retention, and endurance is currently available.[6a] Although there are several types of memory, such as electret,[7] ferroelectric polymer,[8] resistive,[9] and flash,[10] that may be considered suitable, none of them have reached maturity. Electret memories usually require high operating voltages and suffer from long programming times and low charge retention.[7] Ferroelectric polymer memories face problems known from their inorganic counterparts: interface charge trapping, fatigue, and imprint.[8] Resistive memories require currents to operate the memory.[9] Organic flash memories, based on field-effect transistors with a floating gate architecture where charges stored in the floating gate change the threshold voltage of the transistor, currently suffer from either high voltage operation or low charge retention, typically on the order of a few hours or days.[10] In flash memories, the dielectric used to isolate the floating gate from the gate electrode and from the semiconductor is the main problem. The gate dielectric must be dense to achieve extremely low leakage currents, and it must provide very large dielectric breakdown strength.[11]

Here we show that potentiostatically anodized aluminum is a versatile gate and floating gate dielectric for room temperature processed low-voltage non-volatile memories operating below 5 V. Memories were prepared on very different substrate materials: polyethylene naphtalate (PEN), polyimide (PI), and glass. In a hybrid structure with an *n*-octyltrichlorosilane dielectric between the pentacene semiconductor and the aluminum oxide (AlO_x) film on a PEN foil, charge retention larger than 10^5 s is observed.

So far only galvanostatically anodized aluminum has been used in organic field effect transistors.[12] AlO_x is a material with a high dielectric constant, which is between 7.5 and 15, depending on the conditions of preparation.[13] Anodization of aluminum thus promises dense barrier-oxide films with excellent dielectric properties[14] that can be grown on flexible substrates at room temperature. In this work, we use potentiostatic anodization of aluminum to prepare highly reproducible, room-temperature-processed oxide films.

Figure 1a depicts a schematic diagram of the flexible memory element fabricated on a 50 μm thick PEN substrate. Figure 1b shows a top view of a fabricated memory transistor with a channel length L = 75 μm and width W = 2000 μm together with its equivalent circuit, while the photo of the memory element in Figure 1c shows the flexibility of the device. Despite the rather large lateral dimensions of our devices, very promising charge retention times are observed. A reduction in device area (i.e., by the use of smaller shadow masks or photolithographical techniques) is feasible and presumably reduces charge leakage from the floating gate, thus furthermore improving the memory's performance.

As revealed by the transmission electron microscopy (TEM) image in Figure 1d, 15 nm thick Al serves as control gate and an 8.5 nm aluminum oxide layer forms the control gate dielectric. The floating gate consists of a 10 nm thick aluminum layer underlying a 8.5 nm aluminum oxide floating gate dielectric. On top of the aluminum/aluminum oxide multilayer, an *n*-octyltrichlorosilane self-assembled monolayer film is used to form a suitable interface with the organic semiconductor.[15] Such a hybrid dielectric is chosen to improve the leakage currents of the device and to reduce interface traps between the organic semiconductor and the oxide dielectric. 20 nm pentacene forms the organic semiconductor underlying 30 nm thick gold source and drain contacts. The thickness of the whole memory transistor is less than 100 nm in total. For comparison, Figure S1a (Supporting Information) shows a photograph of a memory element on glass, Figure S1b shows the corresponding TEM image, and Figure S1c,d show the electrical characterization of the elements. For the memory elements on glass

M. Kaltenbrunner, Dr. R. Schwödiauer, Prof. S. Bauer
Soft Matter Physics
Johannes Kepler University
Altenbergerstr. 69, 4040 Linz, Austria
E-mail: martin.kaltenbrunner@jku.at
Dr. P. Stadler, Prof. N. S. Sariciftci
Linz Institute for Organic Solarcells
Johannes Kepler University
Altenbergerstr. 69, 4040 Linz, Austria
Prof. A. W. Hassel
Institute for Chemical Technology of Inorganic Materials
Johannes Kepler University
Altenbergerstr. 69, 4040 Linz, Austria

DOI: 10.1002/adma.201103189

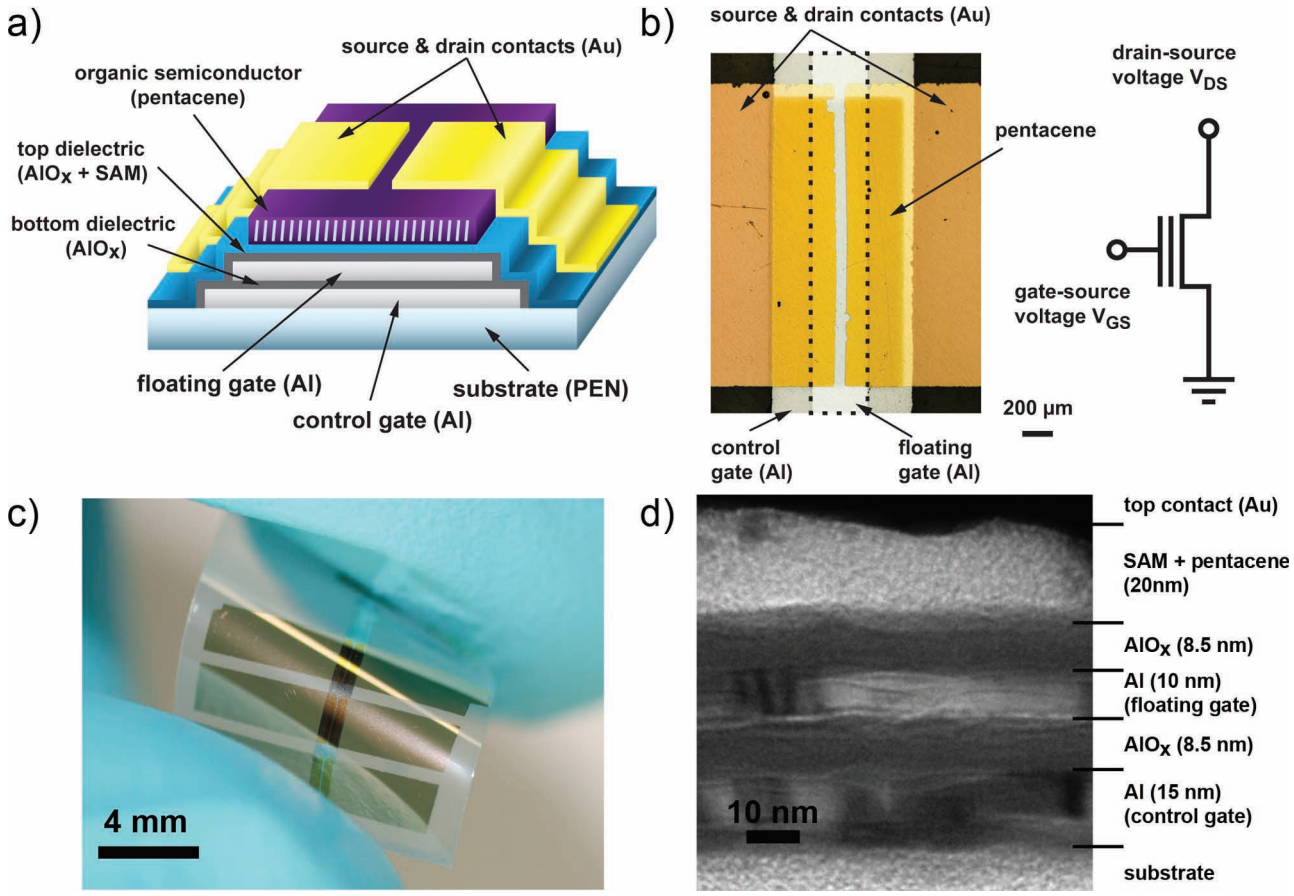

Figure 1. a) Schematic diagram of the non-volatile organic memory element on flexible substrates with a potentiostatically anodized aluminum oxide control gate (8.5 nm) and a floating gate (8.5 nm) dielectric. A *n*-octyltrichlorosilane self assembled monolayer forms the interface to the organic semiconductor pentacene. b) Top-view optical microscopy image of a single-element memory transistor on 50 µm thick flexible PEN with its equivalent electrical circuit. c) Photograph showing the bending flexibility of the memory transistors. d) Cross-sectional TEM image of the floating-gate memory transistor.

divinyltetramethyldisiloxane-bis(benzocyclobutene) (BCB) is used as intermediate layer between AlO_x and pentacene.[16] In the following, we will show similar good performance of memory elements on the flexible substrates (PEN and PI).

Dense, barrier-type aluminum oxide is grown electrochemically by potentiostatic anodization, allowing for precise control of the oxide thickness since the applied anodization potential determines the oxide thickness. Comprehensive details on the potentiostatic anodization of Al are found in ref.[17] and a comparison of leakage currents through anodic barrier oxide films and otherwise formed aluminum oxide can be found in ref.[14]. Potentiostatic anodization seems especially suitable for low-cost, large-area processing of very well defined oxide layers, avoiding high vacuum physical vapor deposition or plasma oxidation. We have used different oxide thicknesses for both gate and floating gate dielectric to demonstrate the adjustability of the memory transistors program/erase voltage (Figure 1d and Supporting Information, Figure S1b).

Figure 2a shows the dielectric properties of the aluminum oxide layers and Figure 2b depicts the tunneling currents through a metal–insulator–metal (MIM) structure with aluminum electrodes and a 8.5 nm thick aluminum oxide dielectric.

The capacitances per area values of the Al-AlO_x-Al structure with 8.5 nm oxide (Figure 2a, black circles) are very high (1040 nFcm^{-2} at 1 kHz). The flat frequency response from 10^{-4} Hz up to 10^{4} Hz shows the good dielectric properties of the prepared layers. This is further corroborated by the dielectric loss tan δ, which is only 5×10^{-2} at 10^{-4} Hz. The same observations hold for the whole floating gate capacitor structure when prepared without the organic semiconductor. Here, a flat capacitance per area of 710 nF cm^{-2} at 1 kHz (grey squares) and a similarly low dielectric loss (at 10^{-4} Hz) are observed.

The current–voltage (*I*–*V*) curve in Figure 2b with a 8.5 nm thick AlO_x layer was measured under quasi-static conditions with an extremely slow sweep rate of 1 mV min^{-1} to minimize effects of slowly decaying von Schweidler relaxation currents.[18] The tunneling current was fitted to the simplest Fowler–Nordheim equation[19]

$$I = \alpha A \frac{a}{\phi} \beta^2 V^2 \exp\left(-\frac{b\phi^{3/2}}{\beta V}\right) \quad (1)$$

where I is the current, V is the applied voltage, and Φ is the work function of the Al-AlO_x junction.

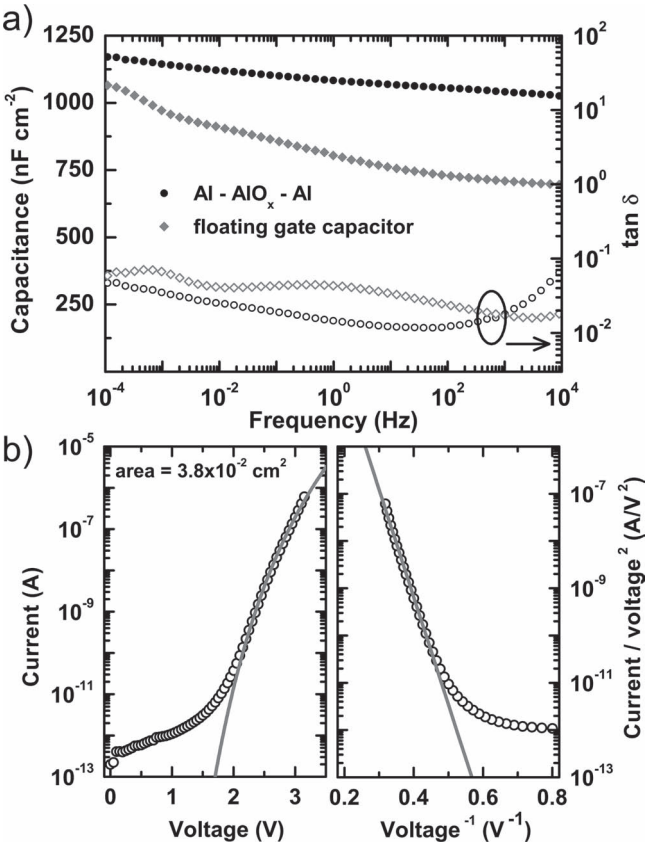

Figure 2. a) Capacitance and dielectric loss angle tan δ of an Al-AlO_x-Al MIM capacitor and a floating gate capacitor on flexible PEN versus frequency. The flat dielectric function and loss indicate excellent dielectric properties of the barrier oxide. b) Tunneling current through an Al-AlO_x-Al MIM capacitor with a 8.5 nm thick barrier oxide versus applied voltage together with Fowler–Nordheim fit (left). Fowler–Nordheim plot of the experimental data and fit (right).

Variables a and b are Fowler–Nordheim constants, given by $a = \frac{q^3}{8\pi h} = 1.54143 \times 10^{-6}\,\mathrm{A\,eV\,V^{-2}}$ and $b = \frac{8\pi}{3}\frac{\sqrt{2m_{ox}}}{qh} = 4.32023\,\mathrm{eV^{-\frac{3}{2}}\,V\,nm^{-1}}$, where q is the elementary charge, h is Planck's constant, and m_{ox} is the effective mass of the electrons in the oxide. For our calculations, an effective mass $m_{ox} \approx 0.4\ m_e$, with the free electron mass m_e, is assumed.[20] For a flat surface, the field conversion factor $\beta = 1/d$, where d is the thickness of the oxide layer. The area of the MIM structure $A = 3.8\ \mathrm{mm^2}$ for the samples in this study. The area is related to the effective field emission area by a factor $\alpha < 1$, suggesting that field emission mainly takes place at localized spots.[18b]

For an average aluminum oxide barrier thickness of 8.5 nm, the work function is $\phi = 1.27$ eV, which is within the range of values reported in ref.[21] Depending on the preparation conditions, electron work functions in the range of 0.9 eV to 2.9 eV were found for aluminum oxide films. The small value of $\alpha = 1.2 \times 10^{-5}$ indicates that field emission arises from a small area only and is probably caused by thickness variations and corresponding field enhancement structures. Below 2 V, the measured currents deviate from the tunneling currents; the values obtained (1 pA at 1 V) are very small. They may be related to hopping conduction in the oxide. They may also be related to leakage currents because we have not observed a clear linear current–voltage relation. We suspect that complex mechanisms in the high-k dielectric AlO_x films are responsible for the observed deviations from the simplest Fowler–Nordheim equation.

Figure S2a,b (Supporting Information) show the dielectric properties of AlO_x on glass, and the I–V curves of the floating gate structure on glass, with a similar value for the work function, a proof for the high reproducibility of the potentiostatically anodized AlO_x on different substrates.

Figure 3a shows the drain current versus gate voltage (black line) after programming the device with –5 V at the gate for 1 s. The grey line indicates the drain current after erasing the memory with +5 V at the gate for 1 s. The drain source voltage was set to 0 V during programming and erasing. A sufficiently large memory window of 2.5 V is observed. Figure 3b depicts the time evolution of the threshold voltage after programming and erasing the memory element. The threshold voltage is obtained using extrapolation in the saturation region.[22] There is a slight change in the threshold voltage shift from –2.8 V at time $t = 0$ to –2.2 V at 10^5 s after programming with –5 V and from –0.4 V at $t = 0$ to –0.8 V at 10^5 s after erasing with 5 V. This is more than an order of magnitude increase in comparison with ref. [10d]. Figure 3c shows the threshold voltages for 10^4 program and erase cycles without visible degradation of the memory window, a promising result in the quest for reliable nonvolatile organic memories. Finally, Figure 3d shows an increase in the obtainable memory window when subsequently applying 100 ms program and erase pulses, suggesting that additional charge is brought onto or removed from the floating gate with every program and erase pulse. Figure S3 (Supporting Information) shows memory elements with BCB as intermediate dielectric between AlO_x and pentacene, fabricated on polyimide foils. A memory window comparable to that of memories on PEN and glass is obtained, with a suitably large memory window for programming at –7 V and erasing at +9 V. Figure S4 (Supporting Information) finally shows that charge trapping at the interface between AlO_x and BCB is negligible, since only transistors (on polyimide) with a floating gate show a memory window when operated through the program and erase voltage levels.

In conclusion, we have shown that potentiostatically anodized aluminum oxide is potentially interesting for the room-temperature fabrication of organic flash memories on rigid and flexible substrates with low, tunable program and erase voltages of –5 V and 5 V, respectively, and a large charge retention time exceeding 10^5 s with only minor degradation of the memory window. Such memories may be useful in flexible electronic devices, which include circuits, sensors, and information storage components.

Experimental Section

To form the control gate, 20 nm of aluminum were vacuum-deposited at a rate of 30 Å s^{-1} onto a 50 µm thick PEN substrate. A 0.01 M citric acid monohydrate ($C_6H_8O_7 \cdot H_2O$) electrolyte was prepared using ultrapure (18 MΩ cm) water. The contacted gates were then immersed into the electrolyte to form the working electrode (anode), and a platinum foil

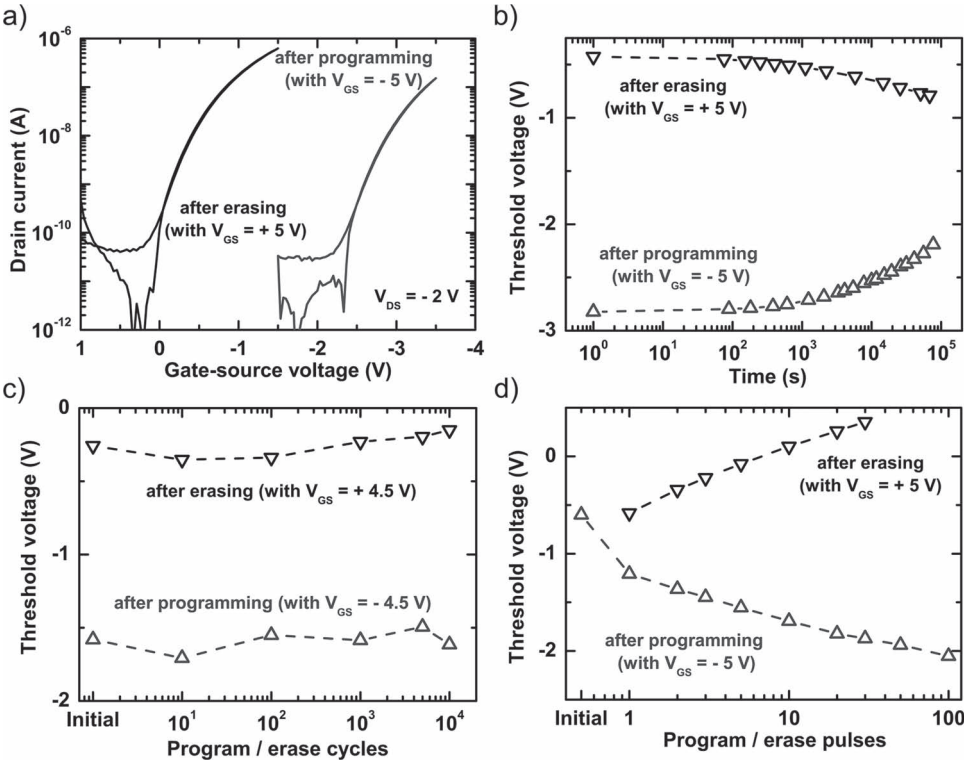

Figure 3. a) Transfer curves after programming with V_{GS} = –5 V for t = 1 s (black curve) and erasing with V_{GS} = +5 V for the same time (grey curve), showing a stable memory window of 2.5 V. b) Time evolution of the threshold voltage after programming (black upward pointing triangles) and after erasing (grey downward pointing triangles), showing a small degradation of the memory window after 10^5 s. c) Memory window versus program and erase cycles; no observable degradation after 10^4 cycles. d) Increase in the obtainable memory window when subsequently applying 100 ms program and erase pulses.

served as counter electrode (cathode). A Keithley 2400 source meter was used as constant voltage source to supply 4 V. The anodization potential was applied for several minutes until the current droped below 1 μA. Approximately 6.4 nm aluminum oxide were grown with an oxide formation factor of 1.6 nm V^{-1}. This resulted in a total oxide thickness of ≈8.5 nm, including ≈2 nm natural oxide that formed immediately upon exposure of the deposited aluminum layer to air. The samples were subsequently rinsed with 18 MΩ cm water and carefully dried in a nitrogen stream.

15 nm of aluminum was vacuum-deposited to form the floating gate on top of the control gate. The subsequent anodization process of the floating gate was carried out in the same way as for the gate electrode; again, 8.5 nm of AlO_x were grown.

An *n*-octyltrichlorosilane self-assembled monolayer was deposited from the vapor phase on top of the floating gate oxide, forming a suitable interface for the organic semiconductor. 20 nm pentacene were grown by hot wall epitaxy at a rate of 0.2 Å s^{-1}.[23] Finally, 30 nm of gold was deposited as source and drain contacts at a rate of 0.2 Å s^{-1}. The channel width W was 2000 μm and the length L was 75 μm.

All memory transistors were characterized using an Agilent E5273A 2-channel-source unit in the dark in a glove box with a dry nitrogen atmosphere. Dielectric measurements were carried out with a Novocontrol Alpha-A High Performance frequency analyzer. *I–V* curves were recorded using a Keithley 6340 A Sub-Femtoamp remote source meter and a custom LabVIEW script.

Supporting Information

Supporting Information is available from the Wiley Online Library or from the author.

Acknowledgements

This work was partially supported by the Austrian Science Funds within the National Research Network on "Interface Controlled and Functional Organic Films". The authors are grateful to Günter Hesser of ZONA for the TEM images and Ingrid Abfalter for helpful discussions.

Received: August 19, 2011
Published online: September 29, 2011

[1] a) H. Klauk, *Chem. Soc. Rev.* **2010**, *39*, 2643; b) D. Braga, G. Horowitz, *Adv. Mater.* **2009**, *21*, 1473; c) S. A. DiBenedetto, A. Facchetti, M. A. Ratner, T. J. Marks, *Adv. Mater.* **2009**, *21*, 1407; d) H. Sirringhaus, *Adv. Mater.* **2005**, *17*, 2411.

[2] H. E. A. Huitema, G. H. Gelinck, J. B. P. H. van der Putten, K. E. Kujik, K. M. Hart, E. Cantatore, D. M. deLeeuw, *Adv. Mater.* **2002**, *14*, 1201.

[3] Y. Kato, T. Sekitani, H. Takamiya, M. Doi, K. Asaka, T. Sakurai, T. Someya, *IEEE Trans. Electron. Devices* **2007**, *54*, 202.

[4] T. Someya, Y. Kato, Y. S. I. Noguchi, T. Sekitani, H. Kawaguchi, T. Sakurai, *IEEE Trans. Electr. Devices* **2005**, *52*, 2502.

[5] a) T. Someya, T. Sekitani, S. Iba, Y. Kato, H. Kawaguchi, T. Sakurai, *Proc. Natl. Acad. Sci. USA* **2004**, *101*, 9966; b) T. Someya, Y. Kato, T. Sekitani, S. Iba, Y. Noguchi, Y. Murase, H. Kawaguchi, T. Sakurai, *Proc. Natl. Acad. Sci. USA* **2005**, *102*, 12321; c) I. Graz, M. Krause, S. Bauer-Gogonea, S. Bauer, S. P. Lacour, B. Ploss, M. Zirkl, B. Stadlober, S. Wagner, *J. Appl. Phys.* **2009**, *106*, 034503; d) S. C. B. Mannsfeld, B. C. K. Tee, R. M. Stoltenberg, C. V. H. H. Chen,

S. Barman, B. V. O. Muir, A. N. Sokolov, C. Reese, Z. Bao, *Nat. Mater.* **2010**, *9*, 859; e) K. Takei, T. Takahashi, J. C. Ho, H. Ko, A. G. Gillies, P. W. Leu, R. S. Fearing, A. Javey, *Nat. Mater.* **2010**, *9*, 821.

[6] a) J. C. Scott, L. D. Bozano, *Adv. Mater.* **2007**, *19*, 1452; b) Q. D. Ling, D. J. Liaw, C. X. Zhu, D. S. H. Chan, E. T. Kang, K. G. Neoh, *Progr. Polym. Sci.* **2008**, *33*, 917; c) W. L. Leong, N. Mathews, B. Tan, S. Vaidyanathan, F. Dötz, S. Mhaisalkar, *J. Mater. Chem.* **2011**, *21*, 5203

[7] a) M. Mushrush, A. Facchetti, M. Lefenfeld, H. E. Katz, T. J. Marks, *J. Am. Chem. Soc.* **2003**, *125*, 9414; b) T. B. Singh, N. Marjanovic, G. J. Matt, N. S. Sariciftci, R. Schwödiauer, S. Bauer, *Appl. Phys. Lett.* **2004**, *85*, 5409; c) K. J. Baeg, Y. Y. Noh, J. Ghim, B. Lim, D. Y. Kim, *Adv. Funct. Mater.* **2008**, *18*, 3678.

[8] a) R. C. G. Naber, C. Tanase, P. W. M. Blom, C. H. Gelinck, A. W. Marsman, F. J. Touwslager, S. Setayesh, D. M. de Leeuw, *Nat. Mater.* **2005**, *4*, 423; b) R. C. G. Naber, K. Asadi, P. W. M. Blom, D. M. de Leeuw, B. de Boer, *Adv. Mater.* **2010**, *22*, 933; c) K. Asadi, D. M. de Leeuw, B. de Boer, P. W. M. Blom, *Nat. Mater.* **2008**, *7*, 547; d) T. Nakajima, M. Nakamura, T. Furukawa, S. Okamura, *Jpn. J. Appl. Phys.* **2010**, *45*, 09MC12; e) R. Kalbitz, P. Frübing, R. Gerhard, D. M. Taylor, *Appl. Phys. Lett.* **2011**, *98*, 033303.

[9] a) M. Colle, M. Buchel, D. M. de Leeuw, *Org. Electron.* **2006**, *7*, 305; b) S. Song, B. Cho, T. W. Kim, Y. Ji, M. Jo, G. Wang, M. Choe, Y. H. Kanhng, H. Hwang, T. Lee, *Adv. Mater.* **2010**, *22*, 5048.

[10] a) K. S. J. Kim, J. S. Lee, *Nano Lett.* **2010**, *8*, 2884; b) M. Burkhardt, A. Jedda, M. Novak, A. Ebel, K. Voitchovsky, F. Stellacci, A. Hirsch, M. Halik, *Adv. Mater.* **2010**, *22*, 2525; c) K. J. Baeg, Y. Y. Noh, H. Sirringhaus, D. Y. Kim, *Adv. Funct. Mater.* **2010**, *20*, 224; d) T. Sekitani, T. Yokota, U. Zschieschang, H. Klauk, S. Bauer, K. Takeuchi, M. Takamiya, T. Sakurai, T. Someya, *Science* **2009**, *326*, 1516.

[11] a) L.-L. Chua, P. K. H. Ho, H. Sirringhaus, R. H. Friend, *Appl. Phys. Lett.* **2004**, *84*, 3400; b) A. Facchetti, M.-H. Yoon, T.J. Marks, *Adv. Mater.* **2005**, *17*, 1705.

[12] a) L. A. Majewski, R. Schroeder, M. Grell, *Adv. Mater.* **2005**, *17*, 192; b) S. Goettling, B Diehm, N. Fruehauf, *J. Displ. Technol.* **2008**, *4*, 300; c) Y. T. Jeong, A. Dodabalapur, *Appl. Phys. Lett.* **2007**, *91*, 193509; d) W. Lin, R. Müller, K. Myny, S. Steudel, J. Genoe, P. Heremans, *Org. Electron.* **2011**, *12*, 955.

[13] M. M. Lohrengel, *Mater. Sci. Eng. R* **1993**, *11*, 243.

[14] D. Diesing, A. W. Hassel, M. M. Lohrengel, *Thin Solid Films* **1999**, *342*, 282.

[15] H. Klauk, U. Zschieschang, J. Pflaum, M. Halik, *Nat. Mater.* **2007**, *445*, 745

[16] P. Stadler, A. M. Track, M. Ullah, H. Sitter, G. J. Matt, G. Koller, T. B. Singh, H. Neugebauer, N. S. Sariciftci, M. G. Ramsey, *Org. Electron.* **2010**, *11*, 207.

[17] A. W. Hassel, D. Diesing, *J. Electrochem. Soc.* **2007**, *154*, 558.

[18] E. von Schweidler, *Ann. Phys.* **1907**, *24*, 711.

[19] a) R. H. Fowler, L. W. Nordheim, *Proc. R. Soc. London, Ser. A* **1928**, *119*, 173; b) R. G. Forbes, *J. Vac. Sci. Technol. B* **1999**, *17*, 526; c) T. W. Hickmott, *J. Appl. Phys* **2000**, *87*, 7903.

[20] T. V. Perevalov, A. V. Shaposhnikov, V. A. Gritsenko, *Microelectron. Eng.* **2009**, *86*, 1915.

[21] a) A. M. Goodman, *J. Appl. Phys* **1970**, *41*, 2176; b) W. H. Rippard, A. C. Perrella, F. J. Albert, R. A. Buhrman, *Phys. Rev. Lett.* **2002**, *88*, 046805–046811; c) E. Cimpoiasu, S. K. Tolpygo, X. Liu, N. Simonian, J. E. Lukens, K. K. Likharev, R. F. Klie, Y. Zhu, *J. Appl. Phys.* **2004**, *96*, 1088.

[22] D. Boudinet, G. L. Blevennec, C. Serbutoviez, J.-M. Verilhac, H. Yan, G. Horowitz, *J. Appl. Phys.* **2009**, *105*, 084510.

[23] A. Andreev, T. Haber, D.-M. Smilgies, R. Resel, H. Sitter, N. S. Sariciftci, L. Valek, *J. Cryst. Growth* **2005**, *275*, 2037.